



ELSEVIER

Thermochimica Acta 261 (1995) 95–106

thermochimica
acta

The thermal decomposition of solid urea hydrogen peroxide

Matthew C. Ball *, Steven Massey

*Department of Chemistry, Loughborough University of Technology, Loughborough,
Leicestershire LE11 3TU, UK*

Received 14 January 1995; accepted 31 March 1995

Abstract

The thermal decomposition of solid urea hydrogen peroxide has been studied at temperatures between 333 and 358 K in flowing nitrogen atmospheres. The decomposition of freshly-prepared material follows Avrami–Erofeyev kinetics, $-\ln(1 - \alpha) = kt^n$, where $n = 2$ at low temperatures and low conversions, and apparently increases with degree of conversion and temperature up to 17 at 358 K. The high values of n are associated with complex melting of the adduct with liberation of oxygen. An activation energy of 113 kJ mol^{-1} for the low- n decomposition has been calculated; the frequency factor is 10^{13} s^{-1} . Aged material decomposes by a phase boundary process with an activation energy of 66 kJ mol^{-1} and a frequency factor of 10^6 s^{-1} . Micrographs are presented which clarify the bulk kinetics.

Keywords: Decomposition; Hydrogen peroxide; Urea

1. Introduction

Solid substitutes for liquid hydrogen peroxide fall into two groups [1]: (a) substituted peroxides, e.g. sodium perborate and peracids; and (b) adducts containing hydrogen peroxide molecules, e.g. sodium carbonate perhydrate, $\text{Na}_2\text{CO}_3 \cdot 1 \cdot 5\text{H}_2\text{O}_2$, and urea hydrogen peroxide, $(\text{NH}_2)_2\text{CO} \cdot \text{H}_2\text{O}_2$ (UHP). These derivatives of hydrogen peroxide have a wide range of uses, from reagents in organic synthesis to detergents [1]. UHP has a high proportion of hydrogen peroxide (36%) and is therefore potentially dangerous. It is available commercially and its use as a reagent in organic synthesis has been described recently [2, 3]. The crystal structure of UHP has been determined [4, 5], and the unit cell is orthorhombic, Pnca, with $a = 6.86$, $b = 4.83$, and $c = 12.92 \text{ \AA}$, and

* Corresponding author.

$Z = 4$. The nitrogen atoms of a urea molecule each makes two hydrogen bonds to hold a hydrogen peroxide molecule in a face-to-face position, and the carbonyl oxygen forms hydrogen bonds to a pair of peroxide molecules. This generates four strings of hydrogen peroxide molecules: two parallel to b and c , and two parallel to a , but at an angle to c . There appears to have been no studies of the thermal decomposition, although the decomposition of the adducts of the alkali metals has been examined [6, 7].

2. Experimental

2.1. Sample preparation

The method of Chia-Si Lu et al. [4] was followed: urea (0.1 moles, 6.0 g) was added to hydrogen peroxide (20 vol., 0.15 moles, 85 ml). The mixture was heated to 330 K and then left to cool and evaporate. Good yields (> 90%) of colourless, elongated prisms were obtained. These were rapidly filtered, air-dried, and then stored at low temperatures over silica gel to avoid decomposition.

2.2. Sample analysis

The hydrogen peroxide content of the solid was estimated by titration with 0.02 M potassium permanganate. The peroxide determined made up > 98% of the theoretical value (36.17%) as long as the crystals were transparent.

2.3. Thermal decomposition

The decomposition studies were carried out using a Stanton Redcroft TG750 thermobalance and a potentiometric recorder. Sample weights were $10 \text{ mg} \pm 10\%$ throughout. Isothermal temperatures were probably accurate to $\pm 1 \text{ K}$. Nitrogen, dried over silica gel and magnesium perchlorate, was passed over the sample at a rate of $5 \text{ cm}^3 \text{ min}^{-1}$.

2.4. Microscopy

The decomposition of the starting material was studied on an optical hot-stage microscope, and crystals heated to various stages of decomposition were examined by SEM (ISI Model SS40) after gold coating. There was evidence of further decomposition in the SEM.

3. Results

3.1. Mass loss

The theoretical mass loss associated with the loss of hydrogen peroxide is 36.17%. Temperatures below 358 K gave mass changes equal to or less than this value, while runs carried out at higher temperatures gave greater changes. The latter were ignored in subsequent analyses.

3.2. Fresh material

All of the experimental mass-loss/time plots for the freshly synthesised material were S-shaped with fairly short initiation periods (Fig. 1). Reduced time plots based on the time for 50% reaction were constructed, and comparison of these with model reduced-time curves based on nucleation, phase-boundary and diffusion control of the reaction allowed a choice of best-fit mechanism to be made [8]. For all of the runs considered, the best fit between experimental and model curves was in terms of the Avrami-Erofeyev equation

$$-\ln(1 - \alpha) = kt^n$$

where α is the proportion decomposed. Closer analysis of the data by means of plots of $\ln(\text{time})$ against $\ln \ln(1 - \alpha)$ showed that the best-fit value of n also varied with the degree of decomposition (Fig. 2). From this figure, the change in slope between the lower and upper parts of the curves can be seen. Fig. 3 shows values of n calculated over two ranges of α , 0.05–0.2 and 0.2–0.9. It can be seen that the low- α values are constant ($n = 2$) up to 353 K, and then increase slightly. The high-range values start at the same value ($n = 2$) and increase rapidly. Optical microscopy showed that the increase in n roughly coincided in temperature with the apparent melting point. Extrapolation of this upper line (Fig. 3) gives a temperature of about 348 K for the beginning of the high values. Reaction rates were calculated from the runs in the temperature range 333–347 K using the low- α data. Fig. 4 shows the derived Arrhenius plot which includes

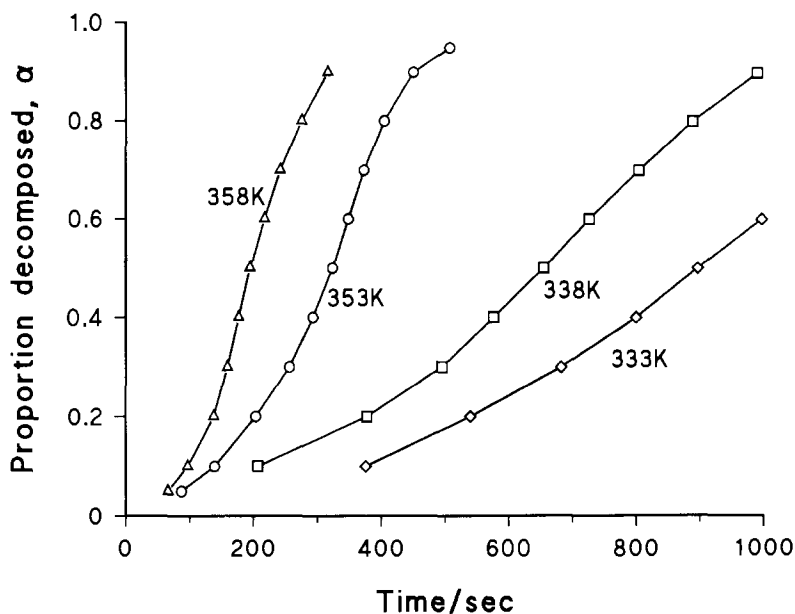


Fig. 1. Decomposition-time curves for UHP.

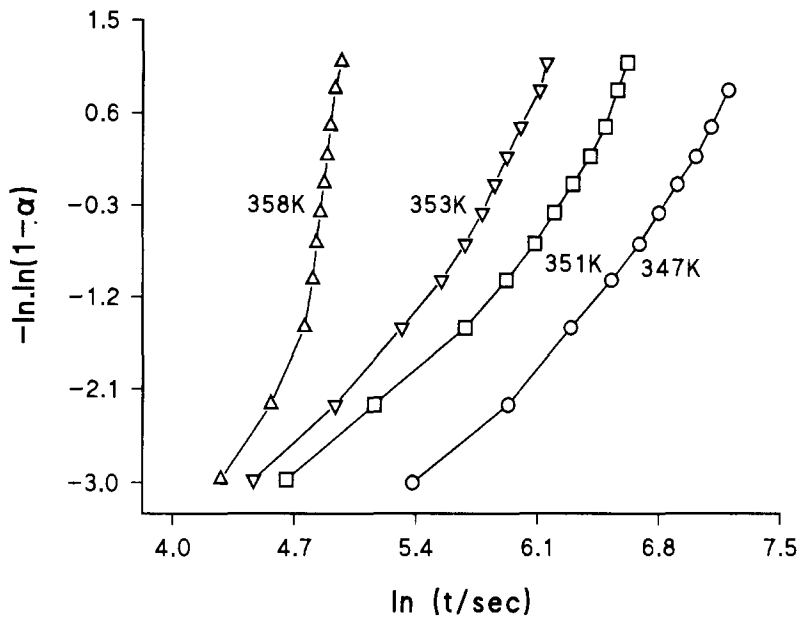


Fig. 2. $\ln \ln(1-\alpha)$ vs. $\ln t$ plots for the decomposition of UHP.

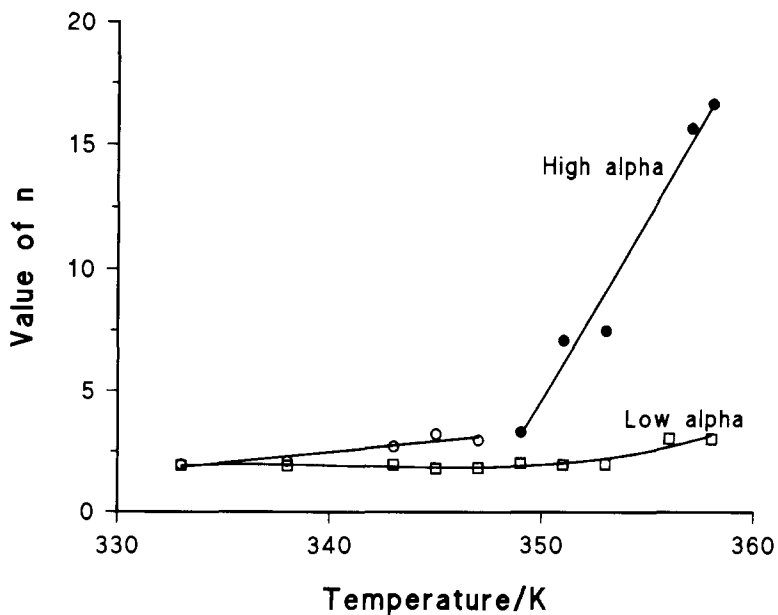


Fig. 3. Value of n vs. temperature for UHP decomposition.

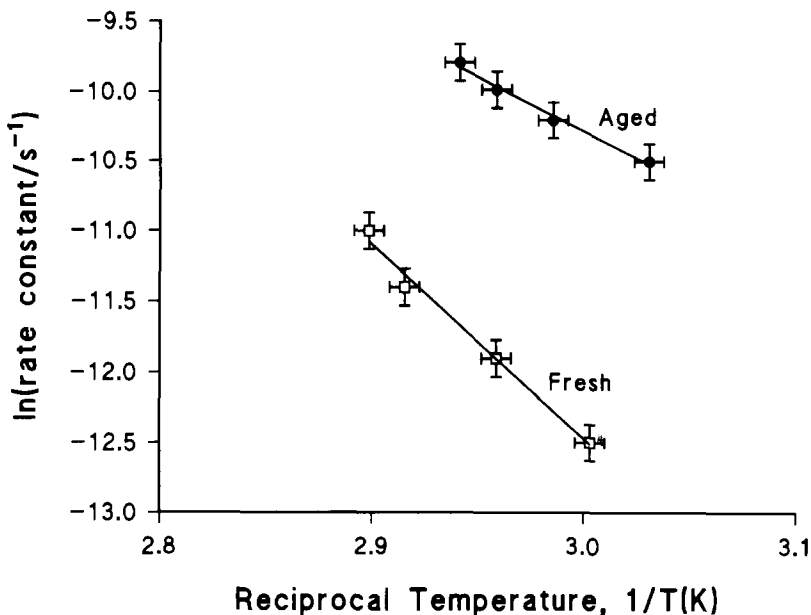


Fig. 4. Arrhenius plot for fresh and aged UHP.

estimates of the experimental errors. The calculated activation energy was $112.7 \text{ kJ mol}^{-1}$, and the pre-exponential factor was $4.8 \times 10^{13} \text{ s}^{-1}$.

3.3. Aged material

A sample of synthetic material was aged by standing in a desiccator at room temperature for 6 h by which time the crystals were opaque. This material contained about 95% of the expected amount of hydrogen peroxide. The decomposition curves for this aged sample were deceleratory throughout, and reduced time plots indicated the best fit between model equations and experimental data was in terms of phase boundary kinetics, following the contracting volume equation

$$1 - (1 - \alpha)^{1/3} = kt$$

Rate constants were again determined and the results are incorporated in Fig. 4. The Arrhenius parameters derived from this give an activation energy of 65.9 kJ mol^{-1} and a pre-exponential factor of 10^6 s^{-1} .

3.4. Microscopy

3.4.1. Decomposition

On gentle heating, the fresh material (Fig. 5) showed small areas of decomposition (Fig. 6), which spread two-dimensionally (Fig. 7). The striations visible on the surface of

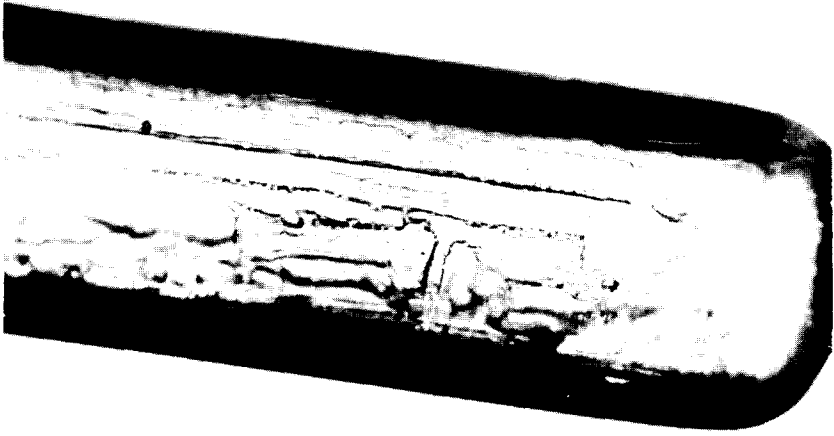


Fig. 5. Fresh UHP, $\times 120$.

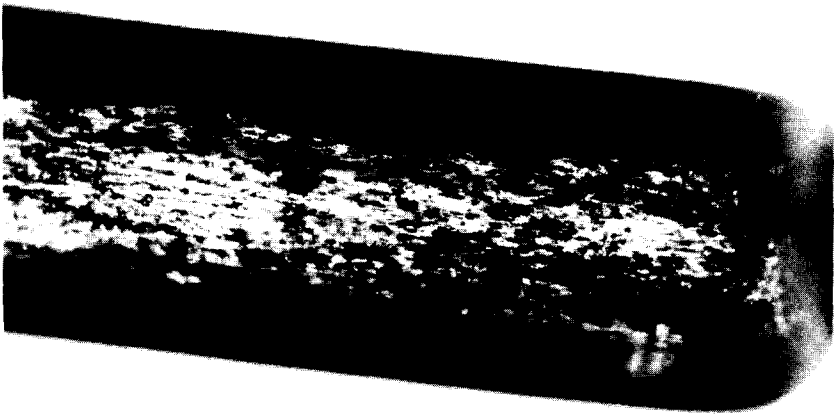


Fig. 6. UHP heated at 325 K, 3 min, $\times 120$.

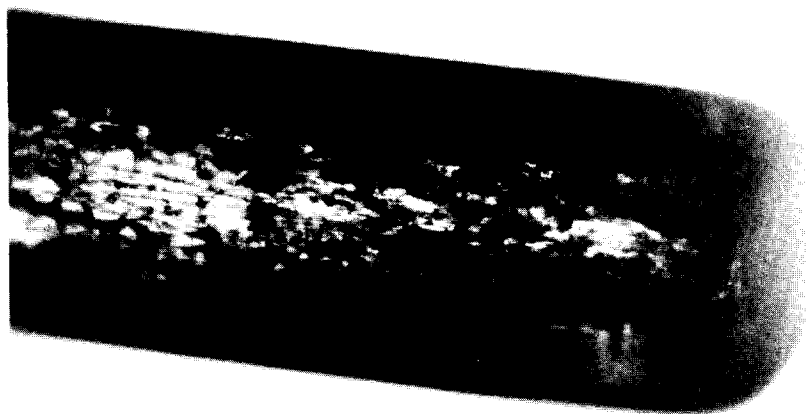


Fig. 7. UHP heated at 325 K, 17 min, $\times 120$.

the original crystal tended to disappear, whilst many of the decomposition nuclei grew along straight lines parallel to the long axis of the crystal. The decomposition nuclei grew rapidly and overlapped to produce opaque crystals. Aligned areas of product were the most obvious feature of the decomposed material when it was examined in the SEM (Fig. 8). This alignment was not uniform on all faces of the product. Figs. 9–11 show three faces of one crystal, and it is clear that there are crystallographic differences in the orientation of the product, urea.

3.4.2. *Melting behaviour at constant temperature*

When crystals were heated at temperatures above about 347 K they rapidly became opaque and then appeared to melt. Crystal edges began to smooth as a first indication of melting, and this was rapidly followed by the formation of clear liquid, with bubbles of gas forming. Gas evolution became much more obvious as the amount of liquid increased. Crystallisation of the melt took place before gas evolution was complete. An example of the formation of large crystals of urea from the melt is shown in Fig. 12. This figure shows that the crystal as a whole has not melted.

4. Discussion

4.1. *Reaction mechanisms*

4.1.1. *Fresh material*

The decomposition appears to follow Avrami–Erofeyev kinetics with a variable value for n . The commonest value observed for this variable is $n = 2$, and this number is

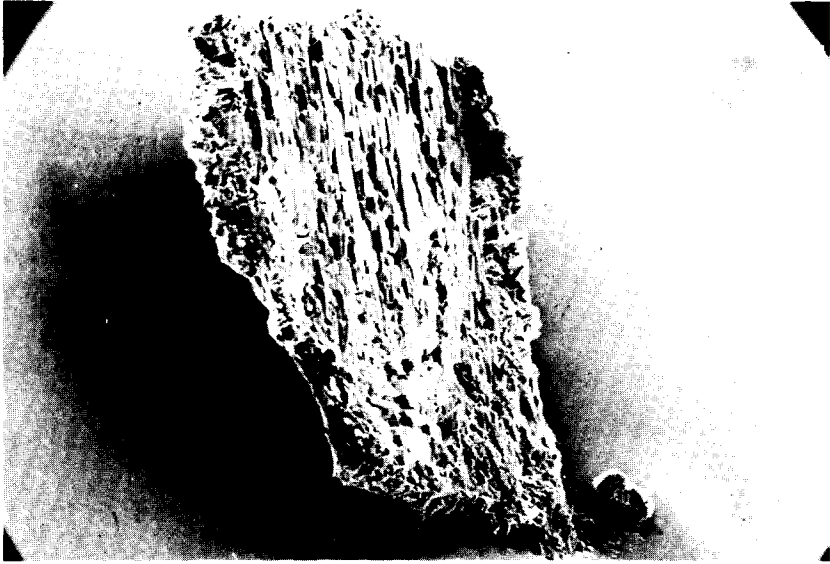


Fig. 8. Fully decomposed UHP, $\times 120$.

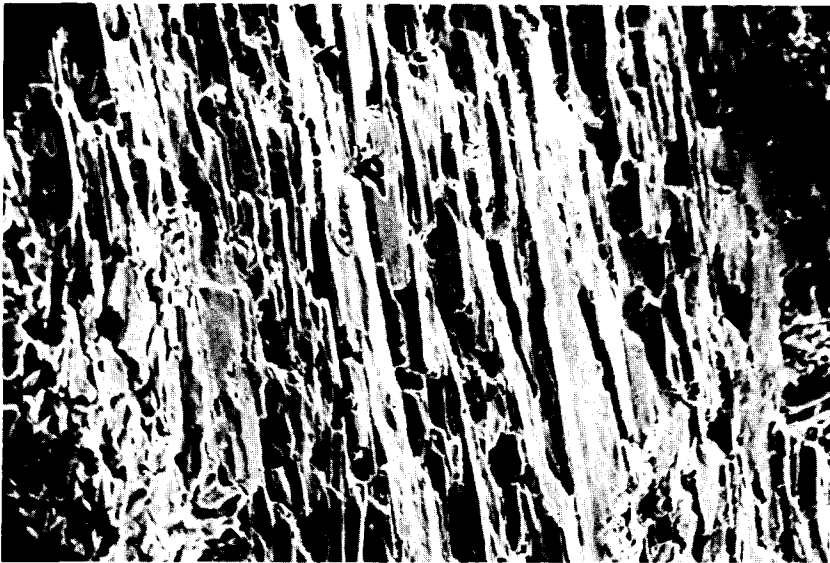


Fig. 9. Fully decomposed UHP, $\times 400$.



Fig. 10. Fully decomposed UHP, $\times 400$.

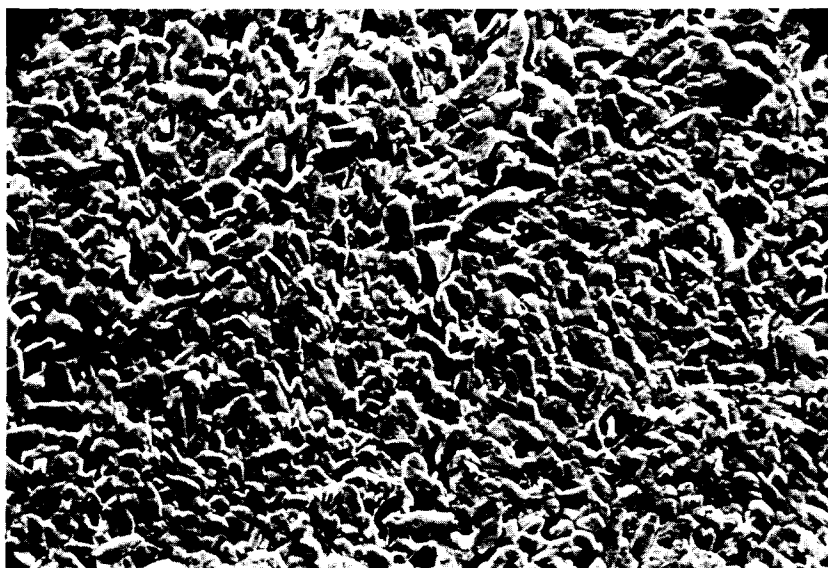


Fig. 11. Fully decomposed UHP, $\times 400$.



Fig. 12. 'Melted' UHP showing large crystals of urea, $\times 120$.

made up of a term for the number of dimensions in which growth is occurring (δ) and another for the time dependence of the nucleation (γ). These give the following possibilities, corresponding to the formation of two-dimensional, one-dimensional and zero-dimensional nuclei

$$n = 2, \quad \gamma = 0, \quad \delta = 2$$

$$\gamma = 1, \quad \delta = 1$$

$$\gamma = 2, \quad \delta = 0.$$

High values of n can normally only come from a rapid increase in the rate of nucleation (γ) with time, given that δ has a maximum value of 3 [9].

Microscopy suggests that the decomposition starts at loci at the surface of the solid, showing as clusters of needles which grow steadily. The surface is rapidly covered with such clusters, most of which seem to start growing from surface imperfections. These clusters could be described as two-dimensional, and all are formed at the start of the reaction, a situation which is best described by the first option above.

The values of $n = 2$ describing the kinetics apply above the apparent melting point of the material. This is an interesting observation and has implications for the mechanism of the melting process (see later).

4.1.2. Aged material

This decomposition followed contracting-cube kinetics (phase boundary control). This is understandable if the aging process has allowed the nucleation stage

to proceed far enough to generate a uniform layer of product across each crystal in the sample.

4.1.3. Arrhenius parameters

The nucleation-and-growth process has a higher activation energy (113 kJ mol^{-1}) which is reduced for the growth process alone (66 kJ mol^{-1}). The pre-exponential factor for the phase boundary process is low, probably indicating a surface transition state [10].

4.1.4. Melting

As mentioned previously, the determination of the kinetics indicated a divergence between the values of n at low and high values of α . These observations, together with the optical microscopy are at least partially accounted for by consideration of the simple binary mixture UHP–urea. True melting does not occur at as low as 347 K, but partial decomposition to urea takes place at this temperature and above, giving rise to the low- α behaviour.

The amount of urea at the crystal surface increases with time, producing a binary mixture with a eutectic of lower melting point than either UHP (melting point unknown) or urea (melting point 405 K). As the decomposition proceeds, the amount of urea increases and the liquidus temperature falls towards the eutectic temperature. If the operating temperature is kept constant, then a liquid phase will be present so long as the operating temperature is above the liquidus temperature. Decomposition is rapid in the melt, because some UPH dissolves, but with this, more urea is formed and the composition of the melt will move towards pure urea. Finally the liquidus temperature will meet the decomposition temperature and the melt will solidify, even though the composition is not that of pure urea. The high values of n obtained at high α -values refer to the evolution of oxygen from the melt, which is much faster than from the solid. The true situation is not as simple as this, because the evolution of bubbles from the melt indicates that the evolved hydrogen peroxide is decomposing to produce water and oxygen. In reality, therefore, the ternary system UHP–urea–water should be considered. The simplest result of having a third phase present would be to make any eutectic temperatures lower than in the binary system. The published phase diagram suggests that liquidus temperatures as low as 307 K might be expected [11].

References

- [1] R. Thompson (Ed.), *The Modern Inorganic Chemicals Industry*, The Chemical Society, London, 1977, pp. 232–272.
- [2] M.S. Cooper, H. Heaney, A.J. Newbold and W.R. Sanderson, *Synlett.*, (1990) 533.
- [3] H. Heaney, *Aldrichim. Acta*, 26 (1993) 35.
- [4] Chia-Si Lu, E.W. Hughes and P.A. Giguere, *J. Am. Chem. Soc.*, 63 (1941) 1507.
- [5] C.J. Fritchie and R.K. McMullan, *Acta Crystallogr. Sect. B*, 37 (1981) 1086.
- [6] See A.K. Galwey and W.J. Hood, *J. Phys. Chem.*, 83 (1979) 1810 and references cited therein.
- [7] B.V. Erofeyev, A.B. Tsentsiper, G.G. Dedova and I.I. Gorelkin, *Izv. Akad. Nauk SSR Ser. Khim.*, 5 (1974) 14; 6 (1974) 5.

- [8] J.H. Sharp, G.W. Brindley and B.N.N. Achar, *J. Am. Ceram. Soc.*, 49 (1966) 379.
- [9] A.K. Galwey, in C.H. Brennan and C.F.H. Tipper (Eds.), *Reactions in the Solid State, Comprehensive Chemical Kinetics*, Vol. 22, Elsevier, Amsterdam, 1980, p. 41.
- [10] H.F. Cordes, *J. Phys. Chem.*, 72 (1968) 2185.
- [11] E. Janecke, *Recl. Trav. Chim.*, 51 (1932) 579.